

Impact of Higher Fidelity Models on Simulation of Active Aerodynamic Load Control For Fatigue Damage Reduction

Brian Resor^{*}, David Wilson^{*}, Dale Berg^{*}, and Jonathan Berg[†]

Sandia National Laboratories[‡], Albuquerque, NM, USA, 87111

and

Thanasis Barlas[§], Jan-Willem van Wingerden^{**}, and Gijs van Kuik^{††}

Delft University of Technology, Delft, The Netherlands

Active aerodynamic load control of wind turbine blades is being investigated by the wind energy research community and shows great promise, especially for reduction of turbine fatigue damage in blades and nearby components. For much of this work, full system aeroelastic codes have been used to simulate the operation of the actively controlled rotors. Research activities in this area continually push the limits of the models and assumptions within the codes. This paper demonstrates capabilities of a full system aeroelastic code recently developed by researchers at the Delft University Wind Energy Research Institute with the intent to provide a capability to serve the active aerodynamic control research effort. The code, called DU_SWAMP, includes higher fidelity structural models and unsteady aerodynamics effects which represent improvement over capabilities used previously by researchers at Sandia National Laboratories. The work represented by this paper includes model verification comparisons between a standard wind industry code, FAST, and DU_SWAMP. Finally, two different types of active aerodynamic control approaches are implemented in order to demonstrate the fidelity simulation capability of the new code.

I. Introduction

The size of wind turbines has been steadily increasing over the past years. Rotors of more than 120 meters in diameter are already in prototype stage. With the intention to lower the cost per kWh, new trends and technological improvements have been primary targets of research and development. One main focus is on developing new technologies capable of considerably reducing ultimate and fatigue loads experienced by wind turbines. Active aerodynamic load control (AALC) is a concept that is currently focusing on fast-acting, high resolution load

^{*} Members of the Technical Staff; Wind and Water Power Technologies Department; MS 1124

[†] Graduate Student Employee; Wind and Water Power Technologies Department; MS 1124

[‡] Sandia is a multiprogram laboratory operated by Sandia Corporation, a Lockheed Martin Company, for the United States Department of Energy's National Nuclear Security Administration under contract DE-AC04-94AL85000.

[§] Ph.D. Researcher, Wind Energy; Faculty of Aerospace Engineering; Kluyverweg 1, 2629 HS

^{**} Researcher, Delft Center for Systems and Control; Faculty of Mechanical, Maritime and Materials Engineering; Kluyverweg 1, 2628 CD

^{††} Professor, Wind Energy; Faculty of Aerospace Engineering; Kluyverweg 1, 2629 HS

control. Ideally, control should be possible for each blade at any azimuthal position and any span-wise station; this control is achieved through use of aerodynamic control devices with embedded intelligence distributed along the span. These criteria imply implementation of efficient, innovative actuators which drive local aerodynamic surfaces. Through the combination of sensors and controllers they provide (feedback) load control. Such concepts are generally referred to as ‘aerodynamic load control’ or ‘smart rotor control’, terms used in rotorcraft research. Lately, aerodynamic load control techniques have been investigated for wind turbines using aeroservoelastic simulation.^{1,2,3,4,5} A recent overview of research in the field is given in Reference [1].

The Wind and Water Power Technologies Department at Sandia National Laboratories (SNL) has performed extensive simulations of several turbine configurations using two control algorithms and has analyzed the results to estimate the benefits of integrating morphing trailing edge technology into the tip region of turbine blades on 1.5 MW and 5 MW machines. Details of this work is found in References [3,4,5,6].

This article is focuses on extended numerical investigations, utilizing two different aeroelastic tools and two different control design approaches, in order to investigate their impact on the prediction of fatigue loads alleviation with the use of active aerodynamic load control techniques.

II. FAST/AeroDyn/Simulink Simulation Details

A brief overview of previous work by researchers at SNL on the topic of full system aeroelastic simulation of active aerodynamic load control technology is provided here.

Turbine component fatigue damage calculations require time-series load histories at the turbine locations of interest at a number of mean wind speeds spanning the entire operating range of the turbine. These load histories are generated with structural dynamic simulations of the turbine performed with the NREL FAST structural dynamics code⁷, utilizing the NREL AeroDyn aerodynamic code⁸ to compute the aerodynamic forces on the blades. FAST utilizes a modal representation of the turbine to determine its response to applied forces. AeroDyn utilizes a combination of the Blade Element Momentum (BEM) and the Generalized Dynamic Wake (GDW) representation of aerodynamic loads, relying on airfoil performance lookup tables to determine the load at any angle of attack. The BEM model is used at wind speeds less than 8 m/s and the GDW model is used for wind speeds of 8 m/s and greater, due to the poor stability characteristics of the GDW model at low wind speeds. AeroDyn contains an important model for dynamic stall based on the semi-empirical Beddoes-Leishman model.

The version of AeroDyn that is used at SNL is modified to model the effects of blade trailing edge deflection by selecting the appropriate lift and drag performance curves in response to flap control input from the controls software. The MatLab/Simulink⁹ control simulation tool is used to model the AALC control logic for the active aerodynamic control simulations. Turbine simulations are typically driven with 10-minute duration, 3-dimensional turbulent wind fields (IEC Normal Turbulence Model¹⁰) generated with the NREL TurbSim code¹¹. The wind files contain an inflow description with appropriate mean wind speed and turbulence content.

Selected load-time waveforms are rain flow cycle counted with the NREL Crunch code¹². The cycles are used in fatigue damage calculations to determine fatigue damage at chosen turbine locations. The impact of active aerodynamic control on the structural loads of the system is evaluated by examining the ratios of baseline rotor and actively controlled rotor damage equivalent loads (DEL) at the chosen locations. The DEL is the single cyclic load amplitude that would produce the equivalent amount of fatigue damage as the entire spectrum of loads that is actually experienced by the structure. An increase in DEL represents an increase in the overall fatigue damage in the structure.

A. Active Aerodynamics Device Modeling

Performance of the active aerodynamic devices are calculated with computational fluid dynamics (CFD). Solutions are obtained over a range of angles of attack using the XFOIL viscous panel code¹³. Solutions are computed for device deflections between +/- 10 degrees in 2 degree increments¹⁴. The raw airfoil tables are then pre-processed using the AirfoilPrep spreadsheet¹⁵, which applies the Viterna¹⁶ method to expand the performance tables to the full

360° range of angles of attack required by the FAST/AeroDyn code. AirfoilPrep also applies a delayed stall model to the airfoils tables to account for blade rotation.^{17,18}

B. Controls Implementation

The active aero load control (AALC) control scheme used in previous work by SNL was a Proportional-Derivative (PD) feedback design that operated completely independently of the standard turbine controller. The PD controller utilizes either blade tip deflection or tip-deflection rate as the feedback. The goal of the controller is to minimize deviation from the reference input signal that represents the behavior of the rotor in steady wind. Simulations assume both sensor availability and ideal sensor feedback from the FAST output with no time delay due to measurement and signal processing.

The active aerodynamic devices are considered to be fast-acting and capable of responding to high-frequency disturbances. Therefore, the integration of the AALC controller with the existing low-frequency blade collective pitch and generator torque control is seamless, with no observed impact of either controller on the other.

In the AALC controller design, the controller gains are selected to optimize device actuation ranges while minimizing blade root flap bending moment oscillations. The movement of the devices are restricted in order to represent what is expected in realistic hardware. Deflection is limited to +/- 10° for the work reported here. The actuator rate is restricted to 100°/s.

Additional information on the development of these control systems may be found in a paper by Wilson et al.³

C. Simulation Improvements

The initial work performed by SNL using the FAST/AeroDyn and Simulink framework suffers from limitations when modeling the wind turbine and the active flap operation. Primarily, limitations include the following:

- The current version of AeroDyn is limited in its ability to represent the unsteady aerodynamics associated with active aerodynamic device actuations.
- The current version of FAST does not include a torsional degree of freedom for the blade structure, so the calculations do not consider torsional deflections due to aerodynamic pitching moments that occur with device actuations.
- The structural model fidelity of FAST is limited in simulation of response of a blade with several independent load control devices distributed spanwise along the trailing edge of the blade. More structural modes of the turbine blades are desired.

An ultimate goal of this research effort is to characterize the impact of load reductions on fatigue damage when independent aerodynamic load control devices and sensors are distributed spanwise along the trailing edge of each blade. The current versions of FAST and AeroDyn are highly effective tools for most turbine system calculations, but are limited in their ability to pursue the work in active device actuation and control for the reasons listed immediately above.

III. The DU_SWAMP Aeroelastic Model

A comprehensive aeroservoelastic tool has recently been developed by researchers at Delft University Wind Energy Research Institute (DUWIND)². Although a variety of widely used aeroelastic codes are available for design, certification and research purposes, the new code has been developed in order to have the advantage of a modular structure, to be able to incorporate realistic effects of distributed trailing edge flaps and to allow for rapid and easy design and implementation of real time controllers. These goals led to the development of DU_SWAMP (Delft University Smart Wind turbine Aeroelastic Modular Processing).

The code is implemented in Matlab and Simulink and comprises a full aeroservoelastic wind turbine model, extended with distributed active control capability features. The structure of the code is fully modular, which offers

the possibility to easily adapt the model configuration and complexity by interchanging modules at any level, as partly illustrated in Figure 1. The implementation of additional features like trailing edge flap aerodynamics models or actuator dynamics behavior is thus facilitated. The model layout also offers the opportunity to use model linearization, system identification and various controller design tools utilizing any available signal in the model. Innovative feedback or feed-forward control schemes based on single-input-single-output (SISO) or multiple-input-multiple-output (MIMO) schemes are easily implemented in DU_SWAMP.

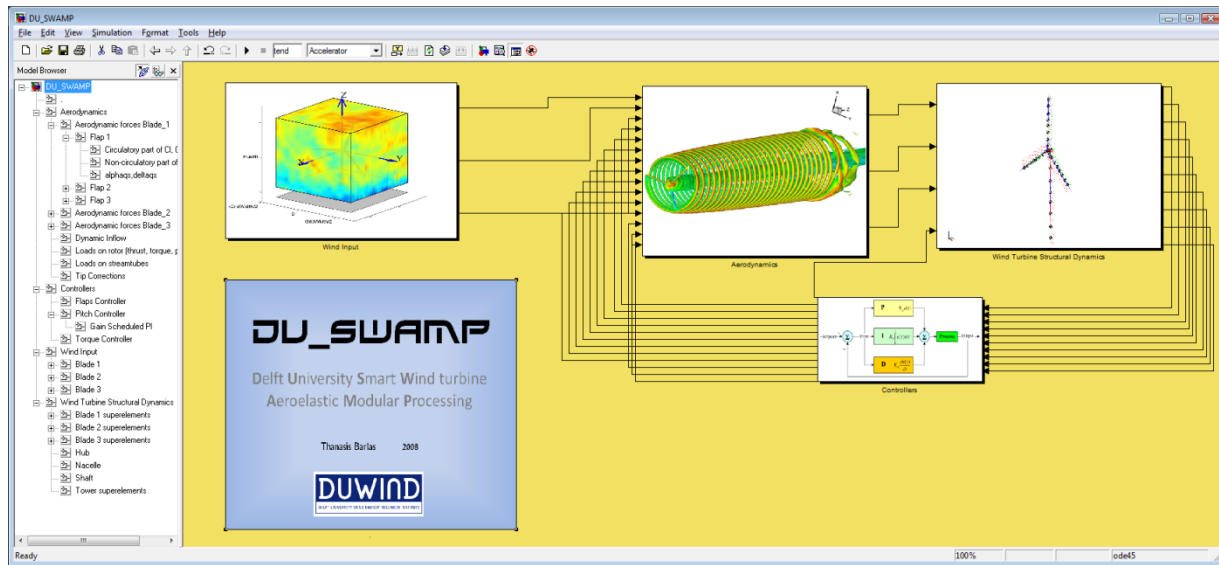


Figure 1. Simulink graphical interface showing sub-modules of the DU_SWAMP code.

The rotor aerodynamics submodel consists of a multiple-streamtube blade element representation coupled with a dynamic inflow model, as described by Snel¹⁹ for the unsteady wake induction. The sectional aerodynamics are described by 2D tabulated data, corrected for 3D effects using the Viterna method¹⁶. For the case of the flapped sections, a 2D unsteady aerodynamic model is used. The unsteady flaps model is based on work for helicopters as described by Leishman.^{20,21} The model analytically predicts the aerodynamic responses of a thin airfoil to arbitrary forcing inputs (airfoil motion, gusts, flap deflection) through an indicial response formulation. Thus, the dynamic effect of a flap actuation is realistically simulated. In fact, the analytical state-space solution is a time-domain representation of the Theodorsen and Wagner function (see Theodorsen²², Wagner²³, and Bisplinghoff²⁴). The model is valid for attached flow conditions. The model has been adapted for wind turbine applications. The general theoretical background is explained with more detail in Reference [2]. The model superimposes unsteady effects due to angle of attack changes, wind gusts, and flap actuations.

The model is modified for this work such that the NREL TurbSim code could be used to generate 3D turbulent inflow as input to the DU_SWAMP simulations. This feature allows direct comparisons of system responses to the same inflow by both FAST and DU_SWAMP. All three components of the variable wind velocity are utilized by the DU_SWAMP aerodynamic models.

The structural dynamics sub-model of the wind turbine is aeroelastically coupled to the aerodynamic model, by means of the structural deformation velocities and the aerodynamic forces. This sub-model consists of a hybrid multibody representation of the wind turbine components. The main flexible structural components (i.e. blades and tower) are represented by superelements (i.e. sets of non-equally distributed rigid bodies connected with linear springs and dampers, see Figure 2). These are connected with other rigid bodies to formulate the full wind turbine multibody structural problem. The concept of superelements is considered more accurate and computationally efficient than the concept of 'lumped-masses' (see Molenaar²⁵, Holierhoek²⁶, Shabana²⁷, and Rauh and Sciehlen²⁸). In this way non-linear deflections can also be simulated. All necessary blade degrees of freedom are included (flap-

wise bending, edgewise bending and torsion, if chosen). The total number of degrees of freedom in the full wind turbine configuration is determined by the number of superelements used per flexible body. In order to capture the first two bending modes of blades and tower, two to three superelements are used. This leads to 40 to 60 degrees of freedom in the full wind turbine configuration.

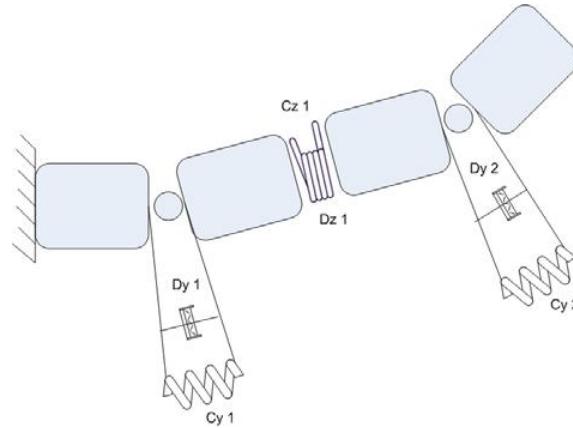


Figure 2. Superelement representation of structural components.

The baseline controllers of the wind turbine are included for power regulation, i.e. generator torque control and above rated full-span pitch control. Any addition of other kinds of load reduction controller, like cyclic or individual pitch control, individual flap control (one flap per blade), or distributed flap control. Virtually any signal can be used for controller input. The actuator dynamics can also be specified in detail, by means of transfer functions, low order dynamic systems, or by setting saturation limits and rate limits for the actuation. This allows for detailed modeling of smart-material based actuation, which has an important impact on the dynamics of the full model.

IV. 5MW Model Description

A full description of the NREL 5MW Offshore turbine model can be found in Reference [29]. The turbine model provides detailed specifications of a large wind turbine that is representative of typical utility-scale land- and sea-based multi-megawatt turbines, and is suitable for deployment in deep waters. The wind turbine is a conventional three-bladed upwind variable-speed variable blade-pitch-to-feather-controlled turbine. Table 1 summarizes the most basic properties of the model used in this simulation. This is a conceptual, rather than an actual, turbine.

Table 1. NREL 5 MW offshore turbine characteristics.

5MW NREL Offshore Turbine Baseline Properties	
Rating	5.0MW
Rotor Diameter	126m
Hub Height	90m
Tower length	107.6m (offshore baseline monopile tower with rigid foundation)
Cut-In, Rated, Cut-Out Wind Speed	3 m/s, 11.4 m/s, 25 m/s
Add-on Active Aero Control Device Properties	
AALC Device	Conventional flap (10% chord)
Extent of flap	About 67% to 91% of blade span, 25% of blade radius
Deflection and rate limits	+/- 10 degrees, +/- 100 degrees/second

DU_SWAMP has the capability to model structural torsion in the blades and tower. However, this feature is not exercised in the current investigation. The first four tower modes are modeled. Three total blade modes are

modeled in FAST: first and second flapwise bending and first edgewise bending. The current DU_SWAMP model accurately represents the first and second structural modes in each orthogonal direction for both the tower and the blades. The following additional physics are not included in the current investigation: drive train dynamics, tower shadow, and aerodynamic hub losses.

V. Baseline Model Comparisons

Sandia National Laboratories and TU-Delft have worked together to verify the DU_SWAMP code against FAST. FAST is chosen as a verification code not because it is believed to represent reality, but because it represents a code that has been used for several active aerodynamic control studies in the past.

Initial verifications consist of baseline models comparisons, utilizing no active aerodynamic devices, throughout the entire range of operational wind speeds. Simulations include operation in both Region 2 and Region 3. Region 2 represents the mode of operation for wind speeds that are above cut-in speed and below rated speed (see Table 1). The collective blade pitch is held constant and generator torque is modulated to control rotor speed in Region 2. Region 3 utilizes both blade collective pitch and torque control to regulate rotor loads to rated specifications. This is the mode of operation when wind speeds are above rated (see Table 1).

Both steady and turbulent wind input cases are used in the comparisons. Initial verifications serve to emphasize the benefits and shortcomings of the simulation capabilities for each model.

D. Steady Wind Input

Initial model comparisons are performed over the full operational range of the turbine. Steady state system response is computed for steady wind speeds at increments of 2 m/s from 5 to 23 m/s. Selected steady wind comparisons are shown in Figure 3. It is important to note that FAST uses the BEM inflow model when average wind speeds are less than 8 m/s and the GDW model when wind speeds are greater than 8 m/s, inclusive.

Rotor thrust predicted by SWAMP is lower than predicted by FAST. The lower thrust predictions by DU_SWAMP here are in line with trends shown in Reference [30]. One explanation is that induction is largely underestimated, which results in higher angle of attack predictions, higher aerodynamic loads, and higher thrust results. Steady wind comparisons performed as part of this work (not shown here) between DU_SWAMP and BLADEMODOE (Energy Research Center of the Netherlands, ECN) show agreement in rotor thrust predictions.

Power coefficient at the lowest wind speeds show discrepancies in predictions at the low end of Region 2. DU_SWAMP uses the simple Glauert empirical correction for high thrust coefficients in the dynamic inflow model. For very low wind speeds, thrust coefficient is very high (in the vicinity of 1.2) and model predictions for induction factors result in unrealistic performance coefficient. FAST also applies the Glauert correction to thrust coefficients. The comparisons in Figure 3 indicate that there may be a difference in the implementation of the correction factors for low wind speeds.

Trends in flapwise tip displacement are in agreement, but magnitudes differ by a small amount, i.e. 10% at 15 m/s. Differences are a result of a combination of factors. The tower top deflection is included by DU_SWAMP in the blade tip displacements. Additionally, we suspect that the overall rotor thrust predictions by FAST are conservative. It is also important to note that the structural representation of the blades in each model have been verified for the first few modes, but differences in the modeling techniques may play a role in blade tip deflection discrepancies.

There is good agreement in flapwise root moment predictions except at the lowest wind speed. Thrust coefficient is high for DU_SWAMP for very low wind speeds. This results in conservative loads being applied to the blades and therefore conservative root moments.

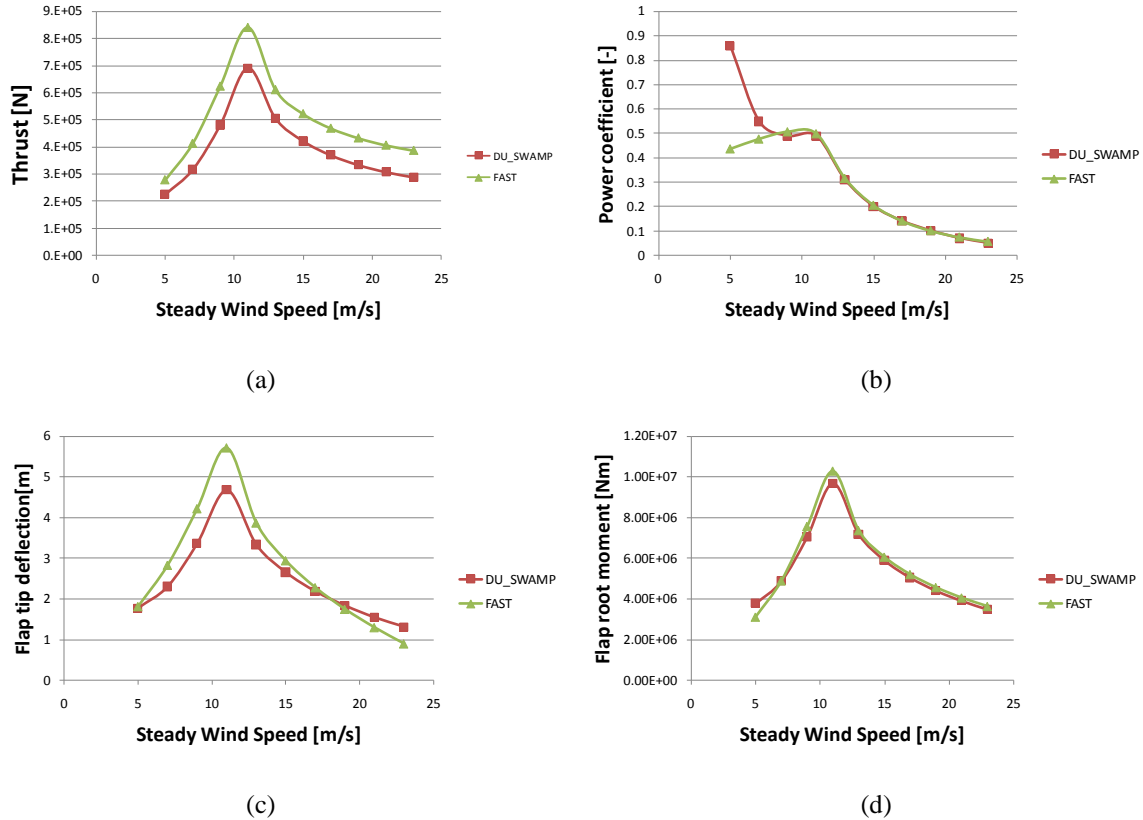


Figure 3. Selected comparisons of model response to steady wind input.

E. Turbulent Wind Input

The next step in model verification compares dynamic response of the models when a three-dimensional full-field turbulent wind input is supplied. The three dimensional wind input is generated by TurbSim with 6% turbulence intensity generated according to the Kaimal spectrum. Six percent turbulence intensity is low compared to typical standards but is chosen in order to ensure the highest reliability of longer simulation runs by DU_SWAMP. Higher levels of turbulence, at this point, cause the Simulink solver used by DU_SWAMP to abort. A working solution to this issue is in development at the time of this writing.

For consistency, the same wind input files are used to excite both the DU_SWAMP model and the FAST model. Four models are compared. FAST/AeroDyn results are shown for both the BEM model and the GDW model. The GDW model differs from the blade element momentum model in that the GDW model is using a Pitt-Peters type of dynamic inflow implementation. This implementation gives time and space varying axial induction factors rather than the steady streamtube based momentum predictions of the BEM model. Both models utilize the Beddoes-Leishman model for dynamic stall.

Two different DU_SWAMP models versions are shown. One model, designated Vinf_average, assumes a constant estimate of hub height wind speed in the calculation of streamtube loads, dynamic inflow, rotor loads, and tip corrections. The other model, designated Vinf_instantaneous, assumes a time-varying estimate of the wind speed at hub height in the same calculations. A full set of simulations are performed for each DU_SWAMP model because preliminary runs in the development process showed dramatic effects of the choice in Region 2.

Selected system response comparisons are shown in Figure 4. Each data point represents the average of ten minutes of simulated operation. Again, it is important to note that FAST automatically switches to the BEM inflow model when average wind speeds are less than 8 m/s and the GDW model when wind speeds are greater than 8 m/s, inclusive.

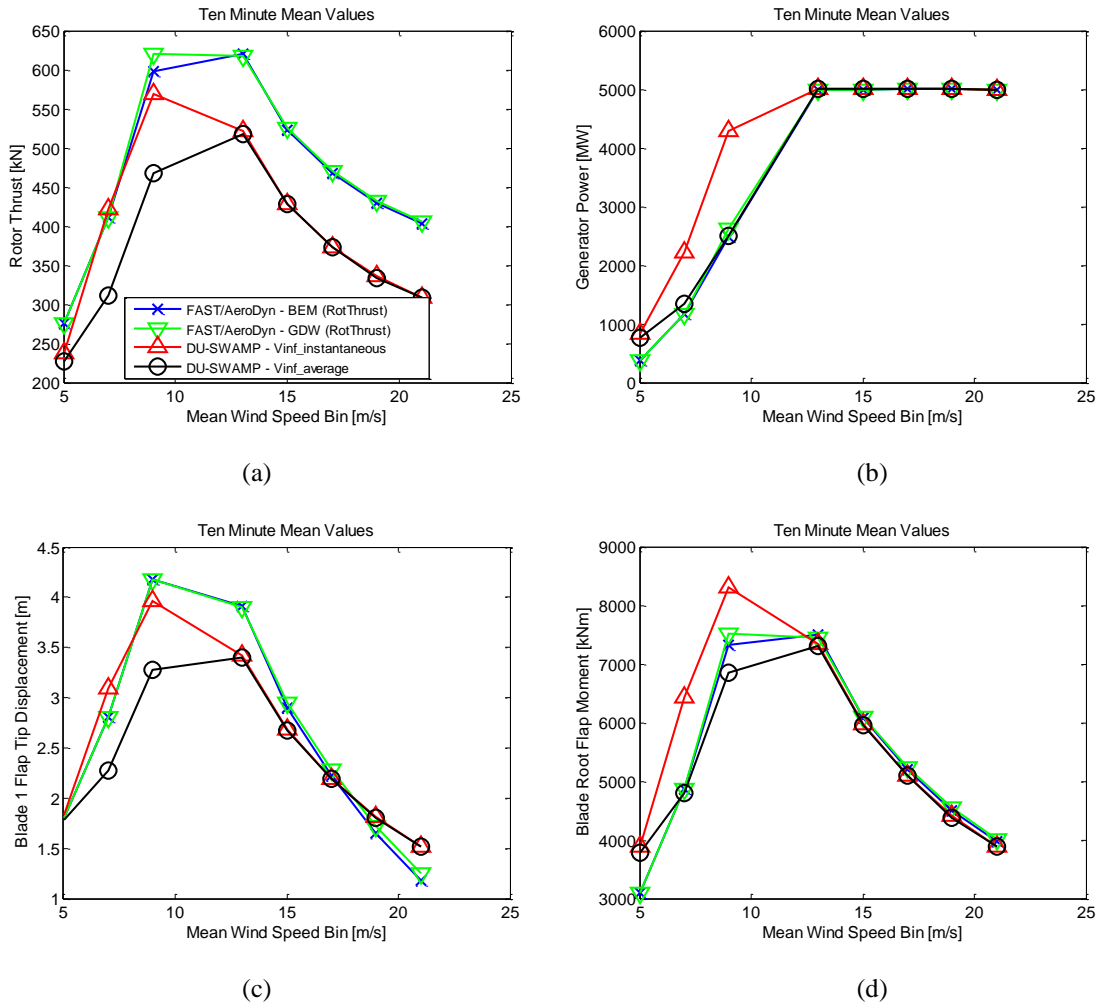


Figure 4. Selected comparisons of model response to turbulent wind input.

Overall rotor thrust predictions by the FAST model are high compared to DU_SWAMP. The same observations are explained in the 'steady wind verification' earlier in this paper. Of particular interest for these turbulent wind simulations is that the rotor thrust calculated by DU_SWAMP when using the instantaneous hub height wind in the analysis is conservative, much like the FAST predictions. This is because the general rotor response with use of Vinf_instantaneous is larger, leading to higher rotor speed and aero forces; therefore, rotor thrust is higher. With the exception of rotor thrust, agreement between models in Region 3 is very good. Proper pitch and speed control algorithms in Region 3 ensure consistent responses. DU_SWAMP power generation in Region 2 is high when the instantaneous hub wind is used. This is because the rotor is experiencing higher torque, as described above.

Predictions of flap tip displacement exhibits similar character and error magnitude as shown in the steady wind comparisons. The sources of the discrepancies are likely similar to what is suggested in the discussion of steady wind results. Root flap moments are in good agreement for Region 3 operation. DU_SWAMP flap moments with

the use of $V_{inf_instantaneous}$ in Region 2 are high. This is due to the fact that the rotor is experiencing higher thrust with the use of the instantaneous inflow measurement.

F. Model Verification Discussion

Many other model comparisons are examined in this work but are not shown here. In general, response comparisons not shown agree well. The responses that have discrepancies are indirectly related to the same issues that are illustrated above in Figure 4. An exception to this is the side-to-side motions and moments associated with the DU_SWAMP tower, which is low in comparison to FAST. Additionally, yaw bearing moments predicted by FAST are low compared to DU_SWAMP. The tower motions due to rotor loading are not discussed in this paper but investigations will be ongoing. Additionally, in the future it will be helpful to output blade tip displacements such that they do not include influence of tower motions.

General dynamic response of DU_SWAMP compares well with FAST. The implementation using the instantaneous hub height wind speed measurement, $V_{inf_instantaneous}$, overestimates the aeroelastic response of the system because aerodynamic loads are higher. This causes excessive values for thrust and torque. The implementation using the constant hub height measurement, $V_{inf_average}$, compares better with FAST overall, with the exception of rotor thrust which is known to be conservative with FAST. FAST and DU_SWAMP $V_{inf_average}$ results for rotor speed in Region 2 are equivalent and rotor loads are truly different between the two cases.

It should be noted that the structural modeling between the two codes is different. FAST uses assumed mode shapes and DU_SWAMP uses multibody super element representations. The current verification work was not designed to highlight any subtle discrepancies that may result from differences in structural modeling approaches. Future work will explore this aspect of increasing the structural model fidelity. Finally, in general, agreement between models in Region 3 is good.

VI. Active Aerodynamics Control Comparisons

Additional simulations exercise the aerodynamic models of the two codes, FAST/AeroDyn in Simulink and DU_SWAMP. Two types of closed loop control schemes are used in the demonstration: 1) a simple PD style controller and 2) a simple high pass filter, to remove the static loads, combined with an inverted notch at the 1P frequency to target the dominant energy in the load spectrum.

Schematics of the two approaches are shown in Figure 5. The objective of the controller is to minimize fluctuations of the blade flapwise tip displacements and, indirectly, blade root loads. The PD controller was exactly replicated in both DU_SWAMP and FAST/Simulink in order to gain an understanding of the differences due to structural representations and aerodynamic flap models. The inverted notch controller is demonstrated only in DU_SWAMP.

Results shown below utilize the DU_SWAMP model with average estimate of hub height wind speed, $V_{inf_average}$. The wind input used in the comparison of active aero control is, as stated above, three dimensional full field turbulent winds with 6% turbulence intensity. A single wind condition in the lower portion of Region 3 at 15 m/s was chosen for the demonstration of active flap control.

Time waveforms for blade flapwise root moments of the baseline and actively controlled rotors are shown in Figure 6. Take away points from this Figure 6 follow. The root moment waveforms have approximately the same mean value and cyclic range is comparable. Waveforms from FAST tend to exhibit a Gaussian-like distribution both before and after implementation of active aero control. DU_SWAMP waveforms tend to exhibit a more triangle-like form both before and after active aero control. This may be attributed to the fact that tower motions play a role in the blade tip deflections that are fed into the DU_SWAMP flap control scheme.

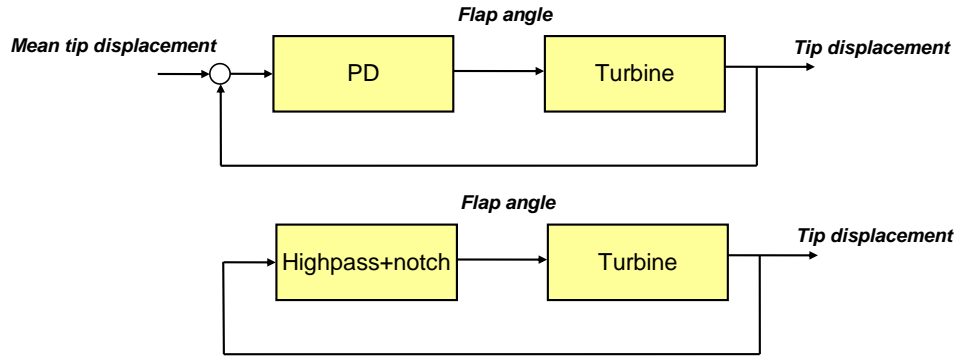


Figure 5. Schematic of two active device control schemes.

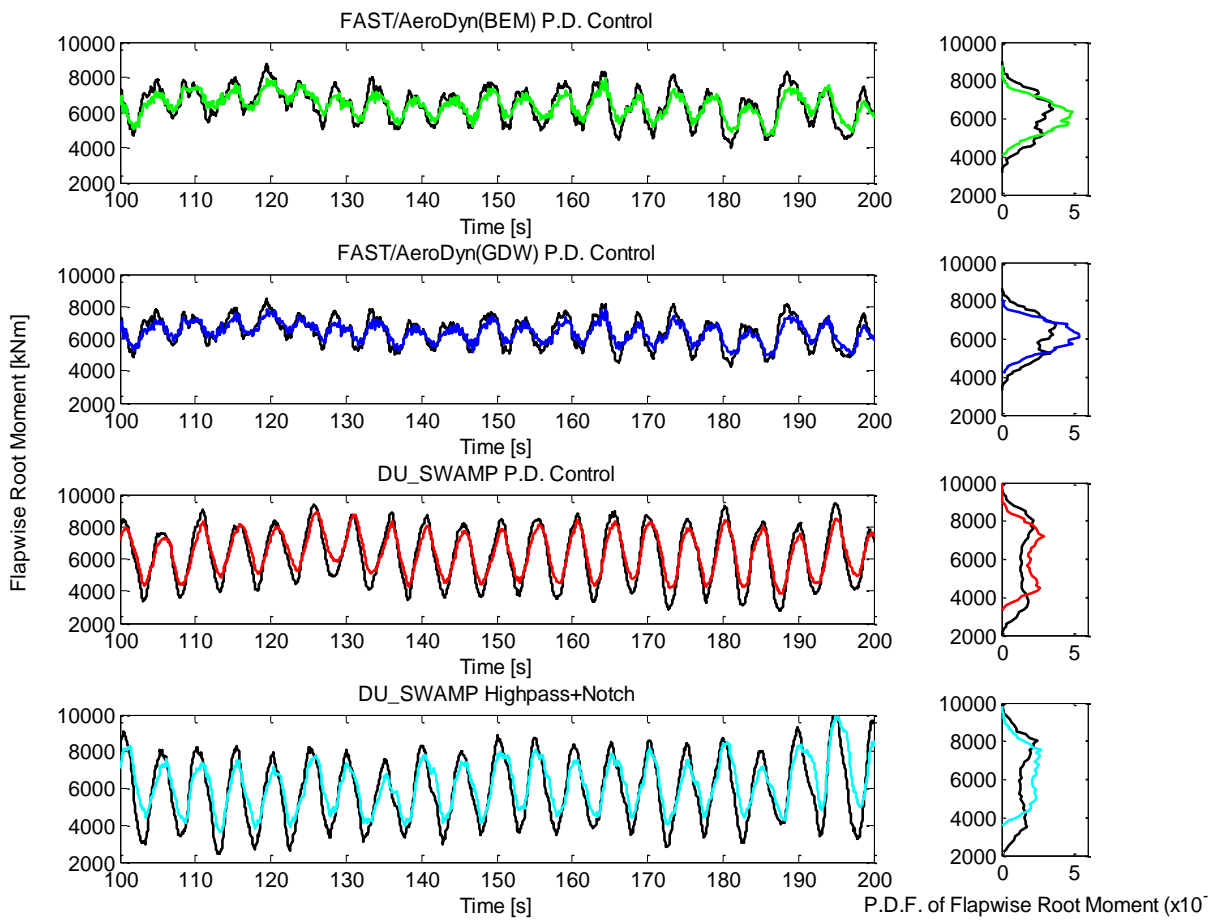


Figure 6. Time domain comparison of baseline responses (black) to responses with active aero PD control (red, blue, green) and highpass filter with inverted notch (cyan).

Figure 7 shows the probability distribution functions (PDF) of flap motions during the active aero control simulations. All control schemes are operating comfortably within the desirable flap actuation range of +/- 10 degrees, with exception of the high pass filter and inverted notch, which saturates at 10 degrees at times. Flap actuation velocities are all similar and do not exceed 50 degrees per second.

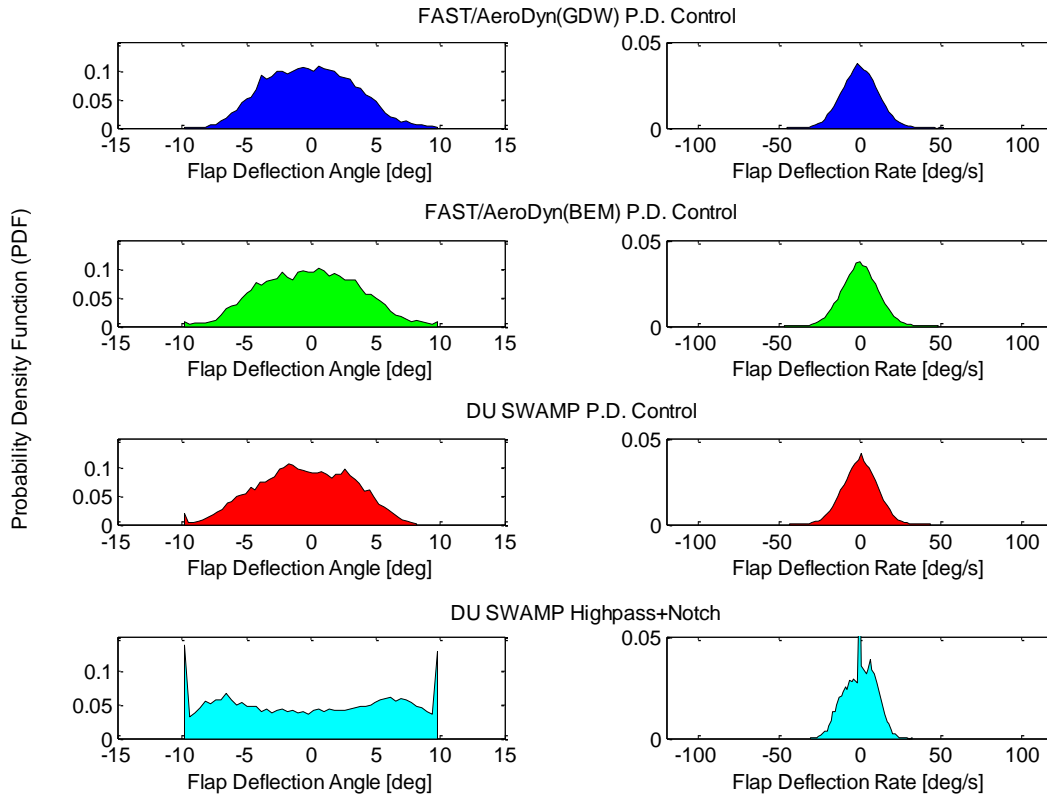


Figure 7. Comparison of active flap motion during active aero control simulation.

The simulation responses are used in a simple fatigue loads analysis in order to arrive at a final estimate of damage equivalent load reductions. Flapwise root moments are rain flow counted by Crunch¹² and results are processed to yield damage equivalent load ratios. Results of rain flow cycle counting are shown in Figure 8. All models show decreases in the cyclic load ranges experienced by the blade root. The fatigue data shown here represents ten minutes of simulation time.

It should be noted that the diversity of cycle amplitudes in Figure 8 would increase as simulated turbulence intensity increases. It will be interesting in the future to examine active flap control with unsteady aerodynamic modeling as the models are able to simulate response to increasing turbulence levels.

Table 2 summarizes load reductions due to active aero control. Reductions in both time waveform standard deviation and damage equivalent load (DEL) are shown. Damage equivalent load reductions are computed for material fatigue exponents of 3 and 10, representing steel and fiberglass, respectively. There is little difference between the two FAST models. The fatigue load reduction benefits for all the cases are similar.

G. Discussion of Flap Aerodynamic Models

Demonstrated fatigue load reductions are similar in all models. However, a close look at the behavior of the flap aerodynamics reveals some of the differences in aerodynamic model behavior. FAST/AeroDyn is using quasi-steady table look-up but also contains a dynamic stall model based on the semi-empirical Beddoes-Leishman model. This feature models the unsteady effects due to changes in angle of attack and (indirectly) wind gusts. DU_SWAMP uses an unsteady aerodynamics model that superimposes unsteady effects due to angle of attack changes, wind gusts, and flap actuations. Comparing the two, we see that the additional capability residing within DU_SWAMP is the ability to include flap actuation effects in the unsteady aerodynamic loads. The unsteady model includes dynamics due to apparent mass effects and shed vorticity, but omits viscous effects that the tabulated data can capture.

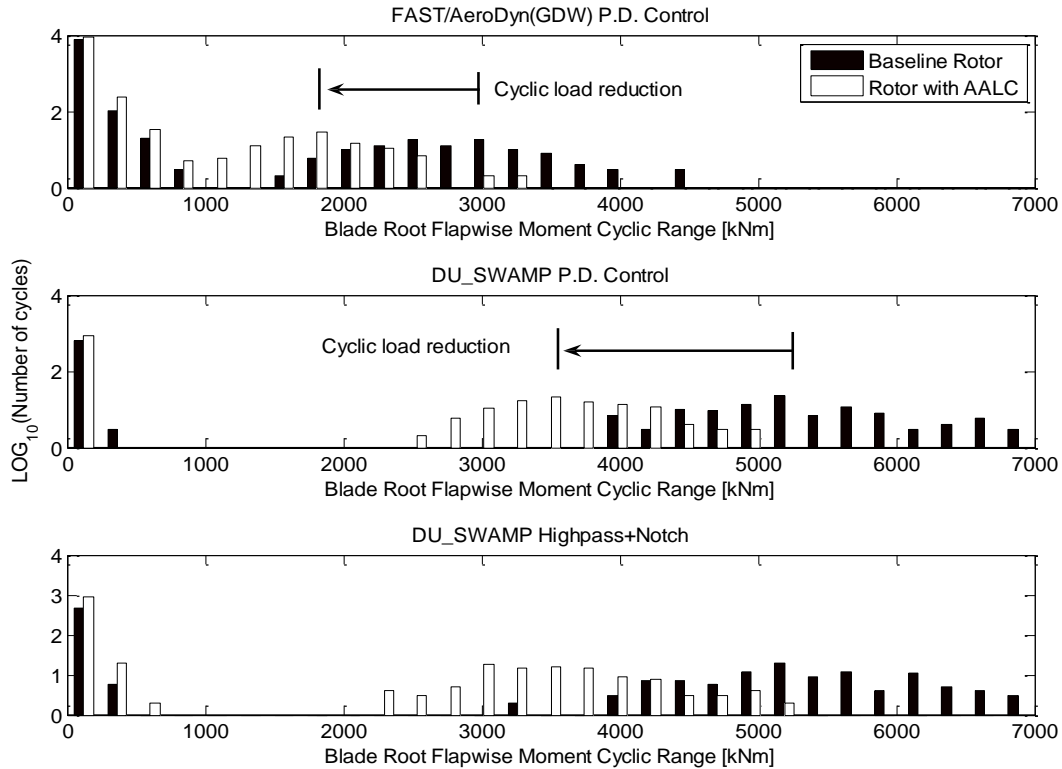


Figure 8. Comparison of rain flow cycle ranges for 600 seconds of simulation. DU_SWAMP & FAST, baseline and active aero PD control.

Table 2. Damage Equivalent Load Reductions in Blade Flapwise Root Moment.

Model Type	Percent reduction in waveform standard deviation, flapwise root moment, 15 m/s	Percent Reduction in DEL, 15 m/s Fatigue exponent, b	
		b = 10 glass composite	b = 3 steel
FAST/AeroDyn with GDW, PD	30.9 %	30.5 %	33.2 %
FAST/AeroDyn with BEM, PD	29.2 %	31.3 %	34.6 %
DU_SWAMP, PD Controller	26.0 %	29.3 %	30.2 %
DU_SWAMP, Highpass+Notch	30.1 %	27.0 %	31.6 %

Figure 9 shows a two-dimensional histogram of aerodynamic flap performance for each model during the 600 seconds of simulation used to produce the load reduction results shown above (startup transient effects ignored). The quasi-steady FAST model simply interpolates aerodynamic performance values from CFD aerodynamic tables of the various flap deflections. The trace of lift coefficient, C_l , and angle of attack in Figure 9 is a relatively predictable path that jumps between the various performance curves of AeroDyn. The unsteady model of DU_SWAMP simulates the transient behavior of C_l for changes in α , resulting in the spreading of C_l data in the graphs.

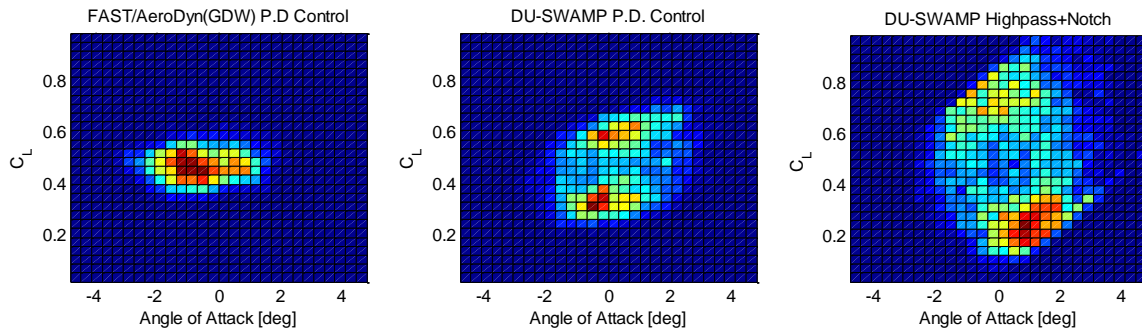


Figure 9. 2D histogram of C_l versus flap section angle of attack in outermost flap section during AALC simulation. Warmest colors (reds) represent regions of highest density of C_l vs. α data.

VII. Conclusions

This investigation provides initial model verifications of the TU-Delft DU_SWAMP full system aeroelastic code against the FAST/AeroDyn code. Comparisons are performed in steady wind and mildly turbulent winds. Initial results show the DU_SWAMP code to be a viable tool for full system aeroelastic simulation in research activities. Ongoing work with the tool will address discrepancies between models that have been noted here.

The current DU_SWAMP model incorporates a different unsteady aerodynamics model than what is currently available in FAST/AeroDyn. The DU_SWAMP model with active aero control demonstrates fatigue load reductions comparable to similar PD control simulations performed with FAST/AeroDyn in Simulink. The aerodynamic models used in the DU_SWAMP model incorporate physics that are more appropriate in simulation of dynamic effects when unsteady flap actuation is present. Additional dynamics included in DU_SWAMP, based on higher fidelity models, are beneficial for controller design, especially when using system identification in the process.

Finally, in this investigation we show preliminary results for a closed loop control scheme that uses a high pass filter with inverted notch. This control scheme performs nearly as well as the simple PD controllers. This scheme is beneficial in that it does not require the knowledge of exact loads or static tip deflections that the PD controller requires. It represents one of many control scheme examples that will be designed and testing in DU_SWAMP in order to advance the state of the art in system control of wind turbine dynamics.

VIII. Future Work

The work presented here outlines some of the initial efforts in evaluating the capabilities of DU_SWAMP and applicability as a research tool for the wind industry. With the capabilities of DU_SWAMP now exercised and understood, additional investigations with these tools by SNL and TU-Delft are ongoing. Some activity will be directed at improving user efficiency of the tool, i.e. documentation, preprocessors for model creation, batch run modes, etc. An important area of further work will center on improving the computational efficiency of the tool. Efforts will focus on implementing the quickest and most accurate means simulation to enable rapid turn-around on design studies. The modularity of DU_SWAMP makes it well-suited for providing a sandbox-like environment in which to try new simulation concepts, i.e. advanced controller development and aerodynamic and wake models. Both of which will be investigated. The structural modeling techniques used in DU_SWAMP, multiple superelements, enable the user to include higher numbers of structural degrees of freedom for studies that need to

understand effects of higher order modes, such as torsion. The effects of these higher modes on control design and operation will be quantified.

IX. References

-
- ¹ T.K.Barlas and G.A.M.vanKuik, Review of state of the art in smart rotor control research for wind turbines, *Prog Aerospace Sci* 46 (2010) 1–27.
- ² Barlas, T.K., and van Kuik, G.A.M., "Aeroelastic Modelling and Comparison of Advanced Active Flap Control Concepts for Load Reduction on the Upwind 5MW Wind Turbine". European Wind Energy Conference, Marseille, France, 16-19 March, 2009.
- ³ Wilson, D.G., Berg, D.E., Barone, M.F., Berg, J.C., Resor, B.R., and Lobitz, D.W., "Active Aerodynamic Blade Control Design for Load Reduction on Large Wind Turbines" European Wind Energy Conference, Marseille, France, 26-19 March, 2009.
- ⁴ Berg, D.E., Wilson, D.G., Barone, M.F., Berg, J.C., Resor, B.R., Paquette, J.A., and Zayas, J.R., "The Impact of Active Aerodynamic Load Control on Fatigue and Energy Capture at Low Wind Speed Sites", European Wind Energy Association, Marseille, France, 16-19 March, 2009.
- ⁵ Berg, D.E., Wilson, D.G., Resor, B.R., Barone, M.F., Berg, J.C., Kota, S. and Ervin, G., "Active Aerodynamic Blade Load Control Impacts on Utility-Scale Wind Turbines" WINDPOWER 2009, Chicago, Illinois, 5-7 May, 2009.
- ⁶ Wilson, Berg, D.E., D.G., Resor, B.R., Barone, M.F., and Berg, J.C., "Combined Individual Pitch Control and Active Aerodynamic Load Controller Investigation for the 5MW UpWind Turbine, WINDPOWER 2009, Chicago, Illinois, 5-7 May, 2009.
- ⁷ NWTC Design Codes (FAST by Jason Jonkman), <http://wind.nrel.gov/designcodes/simulators/fast/>. Last modified 12-August-2005; accessed 12-August-2005.
- ⁸ NWTC Design Codes (Aerodyn by Dr. David Laino), <http://wind.nrel.gov/designcodes/simulators/aerodyn/>. Last modified 05-July-2005; accessed 05-July-2005.
- ⁹ MatLab/Simulink – *Matlab* version 7.8 release 2009a and *Simulink* version 7.3 release 2009a. The Mathworks Inc.
- ¹⁰ IEC TC88-MT1 (ed.). "IEC 61400-1 Ed.3: Wind Turbines – Part 1: Design Requirements", International Electrotechnical Commission, Geneva, 2005.
- ¹¹ NWTC Design Codes (TurbSim by Neil Kelley and Bonnie Jonkman), <http://wind.nrel.gov/designcodes/preprocessors/turbsim/>. Last modified 11-September-2008; accessed 11-September-2008.
- ¹² NWTC Design Codes (Crunch by Marshall Buhl). <http://wind.nrel.gov/designcodes/postprocessors/crunch/>. Last modified 01-April-2008; accessed 01-April-2008.
- ¹³ Drela, M. and Giles, M.B. "Viscous-inviscid analysis of transonic and low Reynolds number airfoils, *AIAA J*, 25(10):1347-1355, 1987.
- ¹⁴ Lackner, M. and van Kuik, G., "A Comparison of Smart Rotor Control Approaches using Trailing Edge Flaps and Individual Pitch Control", 47th AIAA Aerospace Sciences Meeting and Exhibit, Orlando, Florida, 5-8 January, 2009.
- ¹⁵ NWTC Design Codes (AirfoilPrep by Dr. Craig Hansen). <http://wind.nrel.gov/designcodes/preprocessors/airfoilprep/>. Last modified 16-January-2007; accessed 16-January-2007.
- ¹⁶ Viterna, L.A. and Corrigan, R.D., "Fixed Pitch Rotor Performance of Large Horizontal-Axis Wind Turbines", Proceedings of a Workshop on Large Horizontal-Axis Wind Turbines Held in Cleveland, Ohio, July 28-30, 1981, Robert Thresher, Editor, SERI/CP-635-1273 (DOE Publication CONF-810752, NASA Conference Publication 2230). 1982, pp. 69-85.
- ¹⁷ Du, Z, and Selig, M.S., "A 3-D stall-delay model for horizontal axis wind turbine performance prediction", 36th Aerospace Sciences Meeting and Exhibit, Reno, NV, 12-15 January, 1998.
- ¹⁸ Eggers, A.J., Jr., Chaney, K., Digumarthi, R., "An Assessment of Approximate Modeling of Aerodynamic Loads on the UAE Rotor", 41st Aerospace Sciences Meeting and Exhibit, Reno, NV, 6-9 January, 2003.

-
- ¹⁹ Snel H. Survey of induction dynamics modelling within BEM-like codes: Dynamic inflow and yawed flow modelling revisited. *Proceedings of the 39th AIAA/ASME*, Reno, NV, USA, 2001.
- ²⁰ Leishman J G. Unsteady lift of a flapped airfoil by indicial concepts. *Journal of Aircraft* 1994; 31: 288-297.
- ²¹ Leishman J G. *Principles of helicopter aerodynamics*, 2nd edition, Cambridge aerospace series, 2006.
- ²² Theodorsen T. General theory of aerodynamic instability and the mechanism of flutter. *NACA Technical Report 497*, 1935.
- ²³ Wagner H. Über die entsehung des dynamischer auftriebes von tragflügeln. *Z. Angew. Math. U. Mech.*, Vol. 118, 1982; 393-409. Wagner H. Über die entsehung des dynamischer auftriebes von tragflügeln. *Z. Angew. Math. U. Mech.*, Vol. 118, 1982; 393-409.
- ²⁴ Bisplinghoff R L, Ashley H, Halfman R L. *Aeroelasticity*. Addison-Wesley Publishing Co.,1955.
- ²⁵ Molennar D-P. *Cost-effective design and operation of variable speed wind turbines*, PhD Thesis. Delft University Press, 2003.
- ²⁶ Holierhoek J G. *Aeroelasticity of large wind turbines*. PhD Thesis. Delft University Press, 2008.
- ²⁷ Shabana A A. Flexible multibody dynamics: Review of past and recent developments. *Multibody system dynamics* 2001; 1: 189-222.
- ²⁸ Rauh J, Schiehlen W. Various approaches for the modeling of flexible robot arms. *Proceedings of the Euromech-Colloquium 219 on refined dynamical theories of beams, plates and shells and their applications*.1987; 420-429.
- ²⁹ Jonkman, J. Butterfield, S., Musial, W., and Scott, G., "Definition of a 5-MW Reference Wind Turbine for Offshore System Development", National Renewable Energy Laboratory, NREL/TP- 500-38060, February 2009.
- ³⁰ Meng, F., Masarati, P., and van Tooren, M. "Free/Open Source Multibody and Aerodynamic Software for Aeroelastic Analysis of Wind Turbines," *Proceedings of the 47th Aerospace Sciences Meeting and Exhibit*, Orlando, FL, 5-8 January 2009.